ACS APPLIED MATERIALS & INTERFACES

Research Article

www.acsami.org

Supertoughened Renewable PLA Reactive Multiphase Blends System: Phase Morphology and Performance

Kunyu Zhang,[†] Vidhya Nagarajan,[†,‡] Manjusri Misra,*[,†,‡] and Amar K. Mohanty*[,†,‡]

[†]Bioproducts Discovery and Development Centre (BDDC), Department of Plant Agriculture, University of Guelph, Crop Science Building, Guelph, N1G 2W1, Ontario Canada

[‡]School of Engineering, University of Guelph, Thornbrough Building, Guelph, N1G 2W1, Ontario Canada

Supporting Information

ABSTRACT: Multiphase blends of poly(lactic acid) (PLA), ethylene-methyl acrylate-glycidyl methacrylate (EMA-GMA) terpolymer, and a series of renewable poly(ether-*b*-amide) elastomeric copolymer (PEBA) were fabricated through reactive melt blending in an effort to improve the toughness of the PLA. Supertoughened PLA blend showing impact strength of ~500 J/m with partial break impact behavior was achieved at an optimized blending ratio of 70 wt % PLA, 20 wt % EMA-GMA, and 10 wt % PEBA. Miscibility and thermal behavior of the binary blends PLA/PEBA and PLA/EMA-GMA, and the multiphase blends were also investigated through differential scanning calorimetric (DSC) and dynamic mechanical analysis (DMA). Phase morphology and fracture surface morphology of the blends were studied through scanning electron microscopy (SEM) and atomic force microscopy (AFM) to understand the strong corelation between the morphology and its significant effect on imparting tremendous improvement in toughness. A unique "multiple stacked structure" with partial encapsulation of EMA-GMA and PEBA minor phases was observed for the PLA/EMA-GMA/PEBA (70/20/10) revealing the importance of particular blend composition in enhancing the toughness. Toughening mechanism behind the supertoughened PLA blends have been established by studying the impact fractured surface morphology at different zones of fracture. Synergistic effect of good interfacial adhesion and interfacial cavitations followed by massive shear yielding of the matrix was believed to contribute to the enormous toughening effect observed in these multiphase blends.

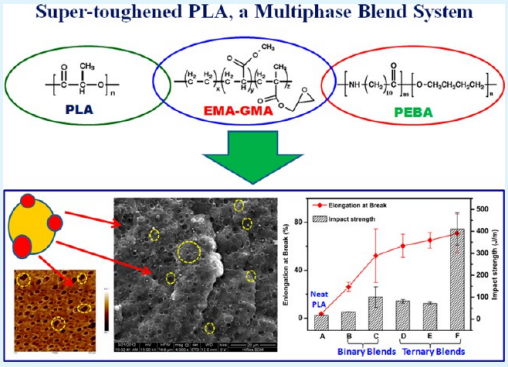

KEYWORDS: *poly(lactic acid), reactive blending, toughness, ternary blend*

1. INTRODUCTION

Poly(lactic acid) (PLA), being a biodegradable polyester derived completely from renewable resources, has attracted a lot of attention in recent years because of its good biodegradability, biocompatibility, high mechanical strength and excellent processability.[1−4] It has been widely researched for use in biomedical applications, such as surgical suture, and drug delivery system.[4] Recently, owing to its affordable performance and availability in the market at a reasonable price, PLA has been considered as a promising and ideal alternative to petroleum-based plastics in commercial applications, such as packaging and fiber materials.[4−6] However, the inherent deficiencies of PLA significantly limit its use in wide range of applications, such as packaging and automotive industries.[6−8]It is well-known that the poor toughness and low heat defection are the major bottlenecks that hinder the applications of PLA in package and automotive industries.[5] PLA exhibits brittleness with only 5% fracture strain in the tensile test, which results in poor impact and tear resistance.[6] Fabricating PLA-based composites is an effective way to improve the heat resistance of PLA materials. However, incorporation of fiber or filler usually further deteriorates the toughness of the materials, which makes it fall short for the required properties for most of the applications. Excellent toughness and flexibility of PLA are the basic prerequisites for developing the PLA composites with desired properties. Therefore, development of the PLA-based materials with high toughness has attracted significant research attention in recent years. Especially, "super-toughness" performance is highly pursued for PLA application areas, mainly for applications in packaging and automotive interior parts.[7,8]

Physical performance of PLA can be improved through several methods including copolymerization, plasticization, and physical blending.[6−8] One of the promising approaches to improve the flexibility and toughness of PLA is blending it with other suitable polymers. Until now, binary blends of PLA with other flexible polymers have widely been reported to improve its toughness and flexibility.[9−23] However, most of the polymers used showed poor miscibility with PLA, which resulted in unsatisfactory toughening effects. As a simple and cost-effective method, multicomponent polymer blends, consisting of at least three components, have attracted a lot

Received: April 17, 2014
Accepted: July 8, 2014
Published: July 16, 2014

attention in modifying the base polymer resin to obtain excellent properties.[24−30] In spite of the large number of studies on the reactive compatibilization or adding compatibilizers for biopolymer binary blends, biopolymer based multicomponent blends have not been widely studied and reported. Recently, some noteworthy results have been reported for PLA-based multicomponent blends with significant improvement in properties. Hillmyer et al. systematically studied a multiphase PLA blend with polyethylene (PE) and a series of PLA−PE block copolymers.[10,11] With the presence of a PLA−PE block copolymer, exceptional toughening of PLA/PE was achieved. Zhang et al. reported super toughened PLA ternary blends from a petroleum-based ethylene/*n*-butyl acrylate/glycidyl methacrylate terpolymer and a zinc ionomer of ethylene-methyacrylic acid copolymer.[31,32] It was suggested that the unique "salami"-like phase structure in conjunction with good interfacial adhesion significantly contributed to the excellent toughness.[32] Zhang et al. investigated renewable and biodegradable ternary blends of PLA, poly(hydroxybutyrate-*co*-hydroxy valerate) and poly(butylene succinate) ternary blends, and found that the blends showed good balanced performance.[33] Favis et al. investigated the phase morphology for a series of ternary biopolymer blends.[34,35] They found that different morphologies could be tuned by changing the components and compositions. These leading works strongly suggest that multicomponent blends are a very effective approach to improve the properties of biopolymers.

Among numerous advantages of PLA, unquestionably, renewable resources based origin is the most attractive feature. Improving the performance of PLA materials without impairing its environmental friendly characteristic is a decisive factor that needs to be considered while selecting materials for PLA modification. From this perspective, suitable elastomeric materials derived from renewable resources will be ideal as modifiers for PLA. Bitinis et al. employed renewable natural rubber (NR) as an effective toughening agent for PLA and its biocomposites.[36−39] It was found that the natural rubber significantly enhanced the tensile toughness of the PLA and the composites. Using in situ X-ray scattering techniques, the deformation mechanism of PLA/NR blend and its composites was studied in detail and analyzed.[37] Poly(ether-block-amide) copolymer (PEBA) is an important class of commercial thermoplastic elastomers with unique physical and processing properties. Recently, Arkema company announced their attempts in making renewable resource based PEBA (Pebax) by combining a biosourced polyol with castor oil chemistry which could reduce fossil-based material consumption and CO_2 equivalent emissions.[40] PEBA is a segmented block copolymer consisting of an aliphatic polyamide as the hard block, a polyether as the soft block and a diacid serving as the joint between the two blocks.[41,42] The unique chemical and segment structure of PEBA offers a wide range of excellent performances including good mechanical properties, biocompatibility and processability, etc. Such excellent properties help PEBA find applications in wide range of fields such as antistatic sheets or belts, food packaging materials and in a variety of medical applications such as short-term implantation in humans and virus-proof surgical sheeting.[41,42] In particular, low glass transition temperature of the polyether-rich phase makes PEBA highly resistant to impact even at temperature as low as −40 °C, and can therefore be used as an impact modifier for the brittle thermoplastic polymers. In view of all these benefits, renewable PEBA is an ideal blending partner for PLA to prepare new environmentally benign material for uses in both biomedical and commodity applications. It is quite reasonable to expect that the introduction of PEBA into PLA may effectively enhance the flexibility and toughness of PLA. Recently, simple binary blends of petroleum-based PEBA elastomer and PLA had been studied.[43−45] It was however found that PEBA/PLA was immiscible and the weak interfacial adhesion resulted in only limited improvement in the toughness of PLA.[44,45]

In the present work, we focused on reactive blending of PLA with a series of renewable resources based PEBA and a functionalized copolymer containing epoxy groups to fabricate supertoughened PLA ternary blends. To the best of our knowledge, the study of PLA and renewable elastomer based multiphase blends have not been reported so far. The phase behavior and mechanical performance of multicomponent blend were thoroughly investigated in the present work. Toughening mechanism in these ternary blends is established by analyzing the relationship between the morphology, thermal behavior and impact toughness of the prepared blends.

2. EXPERIMENTAL SECTION

2.1. Materials. PLA (Ingeo 3251D) with a weight-average molecular weight ($\bar{M}_w$) of 5.5 × 10^4 g/mol and polydispersity index (PI) of 1.62 (GPC analysis) was purchased from Nature Works LLC, U.S.A. PEBA used in this work was purchased from the Arkema Company, having the trade name Pebax Rnew, made of a flexible polyether and a rigid polyamide obtained from renewable resources. Three different grades of PEBA including Pebax Rnew 72R53, Pebax Rnew 55R53, and Pebax Rnew 35R53 were used in the study.

Ethylene-methyl acrylate-glycidyl methacrylate (EMA-GMA) terpolymer containing 8% of glycidyl methacrylate is a product of the Arkema Company with a trade name Lotader AX 8900, obtained from Quadra Chemicals, Canada. Chemical structures of these polymers used for the blends are illustrated in Scheme 1.

Scheme 1. Illustration of the Chemical Structure of the Three Polymers Used

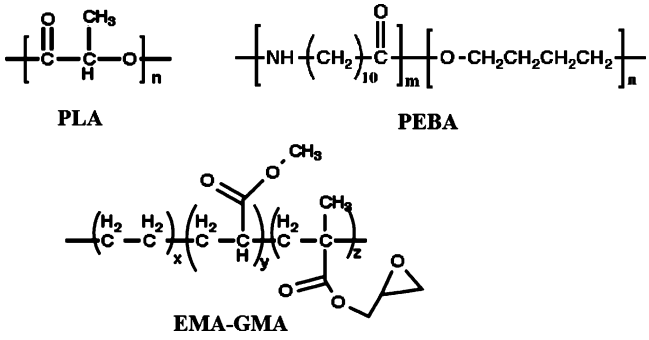

2.2. Preparation of the Blends. Prior to blending, all the materials were dried overnight in the oven, the PLA at 80 °C and the PEBA and EMA-GMA at 60 °C, respectively. Blends of PLA/EMA-GMA/PEBA of varying compositions were melt-processed by a microcompounder (DSM-Xplore, Netherlands). The length and *L*/*D* of the screws are of 150 mm and 18, respectively. The barrel volume of the machine is 15 cm^3. The extrusion was performed at a barrel temperature of 190 °C in a screw speed at 100 rpm. After processing for total 3 min, a preheated cylinder was used to transfer the molten blend material to a preheated injection molder to prepare various test specimens. Also the neat PLA was subjected to the mixing treatment so as to have the same thermal history as the blends.

2.3. Testing and Characterization. *2.3.1. Impact Strength and Elongation.* Notched Izod impact strength was measured with the

help of Testing Machine Inc. (TMI) instrument according to ASTM D256. Tensile properties of the blends were determined by testing the samples on Instron universal testing machine (model 3382) at room temperature, with a tensile test rate of 50 mm/min as per ASTM standard D 638. At least six notched samples were measured for impact strength and 5 samples for tensile strength and elongation. Average values with standard deviations are reported.

2.3.2. Dynamic Mechanical Analysis (DMA). DMA was conducted on a DMA Q800 from TA Instruments using a dual-cantilever clamp with a mode of frequency sweep/temperature ramp at the frequency of 1 Hz and oscillating amplitude of 15 μm. The samples (dimensions 12.7 × 63.5 × 3.2 mm) were heated from −50 to 120 °C at a heating rate of 3 °C/min.

2.3.3. Differential Scanning Calorimetry (DSC). DSC measurements were performed on a TA Q200 DSC instrument under N_2 atmosphere. First, the samples were heated to 190 °C with heating rate of 20 °C/min, followed by isothermal step for 3 min before quenching to −100 °C at a rate of 50 °C/min. The second heating scans were monitored between −100 to 190 °C at a heating rate of 10 °C/min to determine glass transition temperature (T_g), cold crystallization temperature (T'_{cc}), crystallization temperature (T_c), and melting temperature (T_m). Then, the samples were cooled to −100 °C again at a rate of 5 °C/min to characterize the crystallization behavior.

2.3.4. Contact Angle Measurements. The contact angle measurements were obtained using a custom-made system. The system was designed using a fluorescent light bulb, adjustable stage (Newport Optics), an analog CCD camera (EHD imaging) and FlashBus Spectrim Lite framegrabber (Integral Technlologies). The images were processed using the contact angle measurements (CAM) module from the Multiskop software (Optrel) to determine the precise contact angle for each sample that was measured.

2.3.5. Scanning Electron Microscope (SEM). The morphology of the blends was observed using SEM XL30 ESEM FEG (FEI Co.). The samples were cryo-fractured using liquid nitrogen. The fractured specimen was mounted on an aluminum stub using a conductive paint and sputter coated with gold prior to fractographic examination. In addition, to study the detailed phase structure of the ternary blends, the cryo-fractured surfaces were also etched by selectively dissolving PEBA phase in a solvent mixture (1-propanol/1-butanol = 3:1). The solvent extraction was performed at 45 °C for over 48 h under vigorous stirring. Different zones of the specimens' fracture surfaces obtained from notched Izod impact test were also characterized by SEM.

2.3.6. Atomic Force Microscopy (AFM). AFM instrument, Multimode 8 from Bruker Nano Inc., CA, U.S.A., equipped with a Nanoscope V controller and Nanoscope Software, version 8.15, was used for the AFM measurements. Image processing and data analysis were performed using Nanoscope Analysis software. Imaging at Tapping mode and Peak Force Tapping (PFT) Mode was done with RTESPA Si Cantilevers with spring constant of 40 N/m (Bruker AFM probes, CA, U.S.A.) in air. DMT modulus measurements were done by calibrating the cantilevers with fused silica standard sample. PeakForce Quantitative Nanomechanical Property Mapping (PF-QNM) AFM was done at constant oscillation of the sample at 2 kHz using amplitude of 150 nm. The specimens for AFM imaging were prepared by cryo-microtoming with a tungsten knife to create a perfect plane face using Leica Microtome, Germany equipped with a cryo-chamber.

3. RESULTS AND DISCUSSION

3.1. Tensile and Impact Properties. Figure 1 presents the tensile stress−strain curves of the neat PLA, binary blends and PLA/EMA-GMA/PEBA (Pebax 55R53) ternary blends. Figure 2 summarizes the tensile strength and modulus of the neat PLA, the binary blends and the PLA/EMA-GMA/PEBA ternary blends at different wt % formulations. The neat PLA is a brittle polymer with poor ductility and high stiffness. Figure 1 showed that the neat PLA deformed in a typical brittle fashion without obvious yielding under tensile stress. The

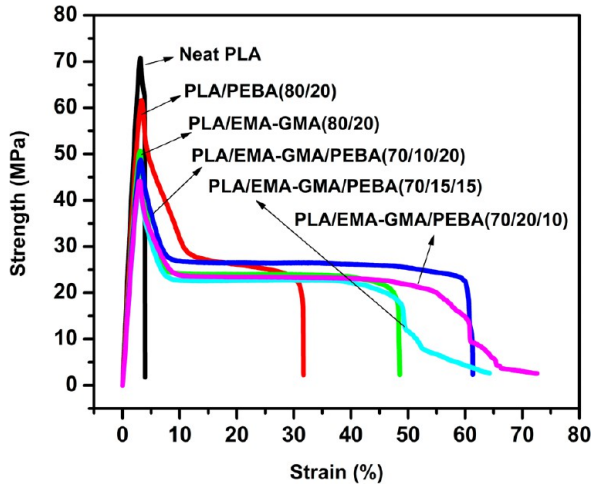

Figure 1. Tensile stress−strain curves of neat PLA, binary blend, and PLA/EMA-GMA/PEBA ternary blends.

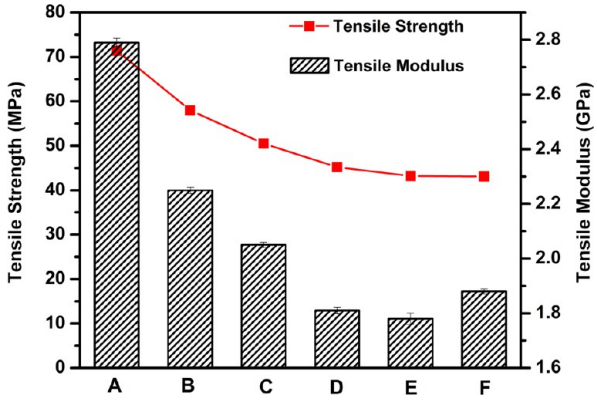

Figure 2. Tensile properties of PLA/EMA-GMA/PEBA ternary blends as a function of the weight fraction: (A) Neat PLA; (B) PLA/PEBA(80/20); (C) PLA/EMA-GMA(80/20); (D) PLA/EMA-GMA/PEBA(70/10/20); (E)PLA/EMA-GMA/PEBA(70/15/15); (F) PLA/EMA-GMA/PEBA(70/20/10).

tensile strength of the PLA was above 70 MPa, while the elongation at break was only around 4%. Compared to the neat PLA, the ductility of PLA was improved by the addition of the PEBA and EMA-GMA elastomers with reduction in strength and modulus. All the blends underwent distinct yielding followed by considerable cold drawing during the tensile test, indicating that the brittle fracture of PLA changed to a ductile fracture with the incorporation of the PEBA and EMA-GMA. At the same time, it is shown in Figure 2 that the tensile strength and modulus of the blends also suffered reduction with the addition of PEBA and EMA-GMA elastomers. The decrease of the strength and modulus for the blends shown in Figure 2 are attributed to the presence of soft PEBA and EMA-GMA elastomers.

Figure 3 summarizes the impact strength and the elongation at break of neat PLA, PLA/PEBA binary blends and PLA/EMA-GMA/PEBA ternary blends as a function of the weight fraction. In the binary blends, the PLA/PEBA (80/20) blend showed increased elongation at break up to 26.2%. During the tensile stress progress, debonding will occur at the particle−matrix interface due to the limited compatibility of the components. The interfacial cavitations caused by debonding create a stress state being beneficial for the initiation of multiple

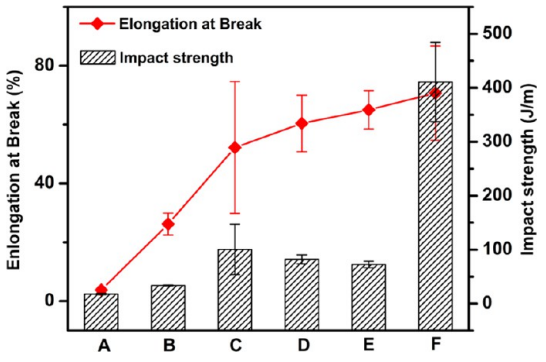

Figure 3. Notched Izod impact strength and percent elongation at break of PLA/EMA-GMA/PEBA ternary blends as a function of the weight fraction: (A) Neat PLA; (B) PLA/PEBA(80/20); (C) PLA/EMA-GMA(80/20); (D) PLA/EMA-GMA/PEBA(70/10/20); (E)PLA/EMA-GMA/PEBA(70/15/15); (F) PLA/EMA-GMA/PEBA(70/20/10).

matrix shear yielding of PLA matrix. Similar tensile phenomena and mechanism was also suggested by Bitinis et al. in the PLA/NR blends and Han et al. in PLA/Poly(ethylene oxide-*b*-amide-12) blends.[37,45] However, as shown in Figure 3, only limited improvement in impact strength was achieved for the PLA/PEBA binary blends. Relatively large size dispersed phases and weak interfacial adhesion of the immiscible PLA/PEBA blend results in the limited improvement in impact strength. Ethylene-acrylic ester-glycidyl methacrylate terpolymers with epoxy group have been widely studied as a single impact modifier for the PLA.[13,14,31,32] While using the EMA-GMA alone as a modifier for the PLA, higher improvement in both elongation and impact strength was achieved compared to the PLA/PEBA (80/20) blend. The improved toughness and ductility can be attributed to the better compatibility of the PLA and EMA-GMA phases, which were also noticed in other works.[13,14,31,32]

Excellent tensile toughness was obtained for the ternary PLA/EMA-GMA/PEBA blends. As shown in Figure 3, all the ternary blend formulations showed higher elongation compared to the neat PLA and binary blends. The elongation at break increased with the increasing content of EMA-GMA in the ternary blend. The PLA/EMA-GMA/PEBA (70/20/10) blend showed the highest elongation of 72.7%, which is almost 20 times higher than that of the neat PLA. Interestingly, it was clearly evident that the impact strength of the ternary blends did not follow the same trend as the elongation. Tremendous increase in the impact strength was achieved in the case of super tough PLA/EMA-GMA/PEBA (70/20/10) blend with a value of 410 J/m exhibiting partial impact break behavior. Yet, the impact strength of the PLA/EMA-GMA/PEBA (70/10/20) and PLA/EMA-GMA/PEBA (70/15/15) blends was found to be even lower than that of PLA/EMA-GMA (80/20) binary blend. These interesting results indicated the materials exhibit different deformation mechanism under different loading conditions of tensile and impact test. It is well-known that the tensile testing is usually performed at a constant low strain-rate condition. However, the impact testing is carried out at remarkably high speed.[19,45] Under the high speed, the notched impact test samples will be very sensitive for the interfacial adhesion. In the PLA/EMA-GMA (80/20) binary blend and PLA/EMA-GMA/PEBA (70/20/10) blend, the different phases showed better interfacial adhesion compared with other formulations. Consequently, they showed higher impact strength. At the same time, it also implied that the phase morphology of the blend played an important role on the toughness of the blends. As discussed in following results, a unique "multiple stacked structure" with suitable interfacial adhesion of the PLA/EMA-GMA/PEBA (70/20/10) played a more effective role in enhancing the impact toughness compared to the other blends.

To develop supertough PLA based blends without greatly sacrificing the stiffness and renewability of PLA, different grades of the PEBA with varying renewable contents and stiffness were also evaluated in two selected ternary blend formulations: the PLA/EMA-GMA/PEBA (70/20/10) and the PLA/EMA-GMA/PEBA (70/10/20). Three typical grades PEBA (Pebax 72R53, Pebax 55R53, and Pebax 35R53) were selected. As reported by the Arkema, the renewable contents and stiffness of the PEBA decrease in the following order: Pebax 72R53 > Pebax 55R53 > Pebax 35R53. Figure 4 summarizes the

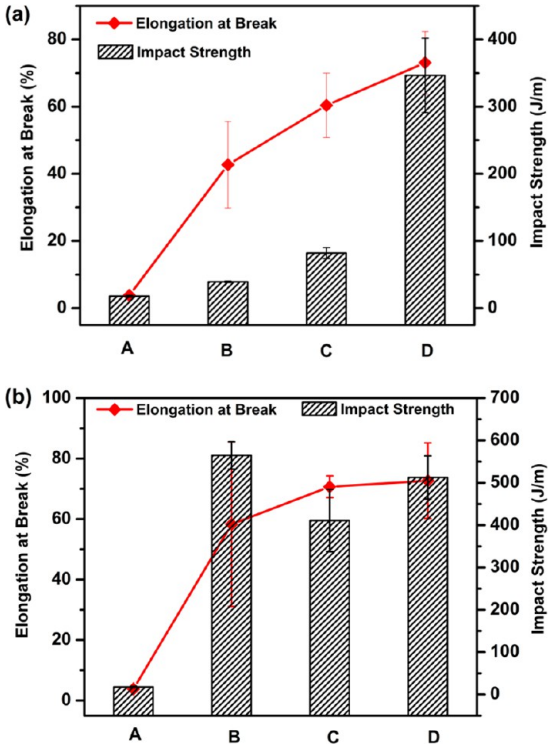

Figure 4. Impact strength and elongation properties of the (a) PLA/EMA-GMA/PEBA (70/10/20) and (b) PLA/EMA-GMA/PEBA (70/20/10) with different grade PEBA: (A) Neat PLA, (B) Blend with Pebax 72R53, (C) Blend with Pebax 55R53, (D) Blend with Pebax 35R53.

mechanical properties of the ternary blends with different grades of PEBA at two selected formulations. In the case of the PLA/EMA-GMA/PEBA (70/10/20) blend with different grades of PEBA, the stiffness of PEBA was found to play a significant role in deciding the toughness and flexibility.

As shown in Figure 4a, the elongation and impact strength increased with the decreasing stiffness of PEBA. However, interestingly, the stiffness of the PEBA showed no big difference in the impact strength for the PLA/EMA-GMA/PEBA (70/20/10) formulation. As shown in Figure 4b, the PLA/EMA-GMA/PEBA 72R53 (70/20/10) blend showed even higher impact strength compared to the blend with low stiffness grade of PEBA. This result is completely different from

the trend observed in the PLA/EMA-GMA/PEBA (70/10/20) ternary blends. This phenomenon suggested that the phase behavior of the ternary blend played an important role in increasing the toughness of the materials and is explained in the later sections.

3.2. Miscibility of the Blends. The miscibility of the components in the blend determines the phase behavior and interfacial compatibility of the blends, which has great influence on the mechanical properties of the materials. Therefore, dynamic mechanical analysis was carried out to assess the miscibility of the polymer blends. Figure 5a and b shows the

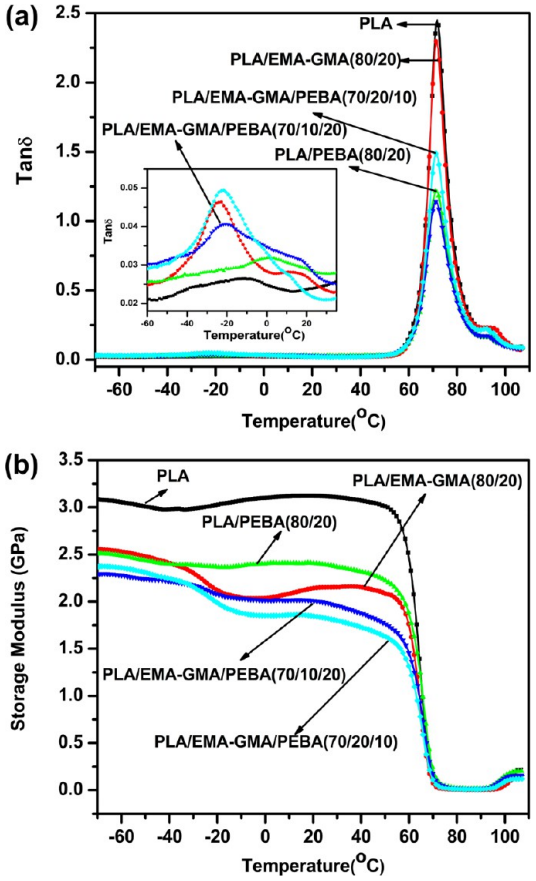

Figure 5. DMA traces of PLA blended with PEBA (Pebax 55R53) elastomer at various concentrations: (a) tan δ versus temperature; (b) storage modulus versus temperature curves.

Tanδ and storage modulus (E') curves of the neat polymers and the blends. As shown in Figure 5a, the neat PLA exhibited a Tanδ peak at about 71.8 °C, which was ascribed to its glass transition. The peaks shifted slightly toward each other for the PLA/EMA-GMA binary blend, indicating the partial miscibility between the components. For the PLA/PEBA binary blends, no obvious change in the peak temperature was noticed, suggesting the poor miscibility of the PLA and PEBA. In addition, a huge difference between the peak intensity of the blends was observed. The PLA/EMA-GMA binary blend showed higher peak intensity compared to the PLA/PEBA binary blend with the same amount of PLA content in the blends. This result suggested that the amorphous part of PLA in the PLA/EMA-GMA binary blend was higher than the PLA/PEBA binary blend. It indicated that the presence of the EMA-GMA more effectively confined the crystallization of PLA due to the optimum level of compatibility between the phases.

As for the ternary blends, it was noticed that the T_g values of both the EMA-GMA and PEBA components in the blends shifted to high temperature, especially for the PLA/EMA-GMA/PEBA (70/20/10) blend. This result indicated the improved miscibility, which could most likely be due to the reaction between the glycidyl methacrylate (GMA) group with the end function group of the PLA and PEBA. During the high temperature melt processing, the chemical reaction between GMA groups on the reactive elastomer and the terminal carboxyl and hydroxyl groups of polymer such as the PLA and PEBA has been clearly identified in the literatures.[15,16,31,32,46,47] In the studies of the PLA/EMA-GMA binary blend, Li et al.[46] and Jiang et al.[47] have clearly confirmed reaction between the epoxy group of the EMA-GMA and terminal carboxyl and hydroxyl groups of the PLA through the direct FTIR evidence. As pointed out by Zhang et al. in their studies,[31,32] the reaction between the terminal carboxyl group of the PLA and the epoxide groups in the EMA-GMA was the major possible compatibilization reaction at the present processing temperature. Compared to the ring-opening synthesized PLA, the carboxylic acid/epoxy reaction has also been well established and widely used for reactive compatibilization for condensation-polymerized polymers such as PEBA.[48] Consequently, in the PLA/EMA-GMA/PEBA ternary blends, the EMA-GMA played unique dual roles as an effective toughening agent and a reactive compatibilizer, which significantly improved the toughness of the PLA blends. The improved compatibility of the EMA-GMA phase with the PLA and PEBA phases was also clearly demonstrated in the following SEM and DSC results.

Figure 5b shows the storage modulus curves of the neat polymer and the blends. The glass transition of the neat PLA started at 50–60 °C, and the storage modulus decreased sharply. The cold crystallization was observed to occur at around 135 °C and as a result of the cold crystallization, the storage modulus increased. In accordance with the tan δ curve, no obvious change in the transition temperature of the PLA was observed in the PLA/PEBA blend due to the immiscibility of the two components. However, the cold crystallization temperature of PLA in PLA/EMA-GMA binary blend and the ternary PLA/EMA-GMA/PEBA blends shifted to high temperature, which was consistent with the following DSC results. This result indicated that the crystallization of PLA was confined in these blends. The E' of the blends decreased at the room temperature due to the soft EMA-GMA and PEBA introduced in the blends.

3.3. Thermal and Crystallization Behaviors. Both the PLA and PEBA are semicrystalline polymers. The physical properties of the PLA are greatly dependent on the solid-state morphology and its crystallinity.[15,44] Accordingly, to make clear conclusions on the mechanism involved in improving the toughness, it is important to study the thermal and crystallization behavior of the blends, especially the crystallization behavior of the PLA phase. Figure 6 presents the melting behavior of the neat PLA and blends after quenching. Figure 7 shows the crystallization curve of the neat PLA and ternary blends at cooling rate of 5 °C/min. The detail results of DSC are summarized in Table 1, which mainly shows the thermal behavior of the PLA in the blends.

As shown in Figure 6, the cold crystallization peak of the PLA in the blends was noted to shift toward high temperature, especially for the PLA/EMA-GMA (80/20) and the PLA/

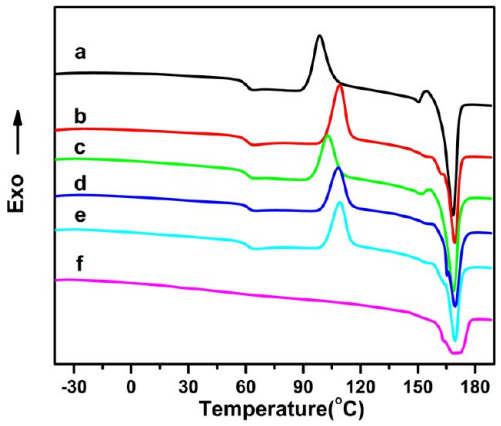

Figure 6. DSC heating curves of the neat PLA and the blends after quenched: (a) neat PLA ;(b) PLA/EMA-GMA (80/20); (c) PLA/PEBA (80/20); (d) PLA/EMA-GMA/PEBA (70/10/20); (e) PLA/EMA-GMA/PEBA (70/20/10); (f) neat PEBA (Pebax Rnew 55R53).

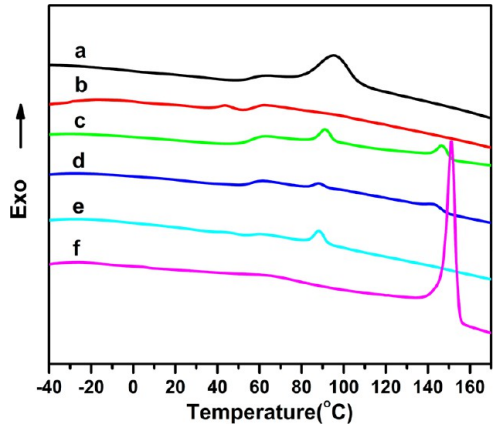

Figure 7. DSC cooling curves of the neat PLA and the blends: (a) neat PLA; (b) PLA/EMA-GMA(80/20); (c) PLA/PEBA(80/20); (d) PLA/EMA-GMA/PEBA(70/10/20); (e) PLA/EMA-GMA/PEBA-(70/20/10); (f) neat PEBA(Pebax Rnew 55R53).

EMA-GMA/PEBA (70/20/10) blends. At the same time, no clear exothermal peak attributed to crystallization of the PLA was observed in Figure 7 for the PLA/EMA-GMA (80/20) blend, which was consistent with the DMA results. For the ternary blends, it was also found that the crystallization temperature of the PLA shifted to low temperature with the increase of the EMA-GMA contents. These results indicated that the presence of the EMA-GMA decreased the ability of the PLA to crystallize. The confined crystallization behavior of the PLA/EMA-GMA blend may suggest the good compatibility of the two components. As discussed in the previous section, the EMA-GMA and PLA showed partial miscibility due to the reactive processing at high temperature. The interaction between the EMA-GMA and PLA segments will confine the crystallization of PLA because of the dilute effect of the EMA-GMA phase. In contrast, for the PLA/PEBA (80/20) binary blend with poor miscibility, the crystallization of the PLA was not influenced apparently. The thermal behavior of PLA in the blends indicated the different miscibility among the components in the blends. At the same time, it was also noticed that the crystallization of the PEBA was confined in the blends. This result indicated that there was segment interaction among the different phases which changed the thermal behavior of the components. The DSC results in accordance with the DMA and SEM results further verified the miscibility of the EMA-GMA with the PLA or PEBA phases.

3.4. Impact Fractured Surface Morphology of the Blends. To further study the toughening effect of the PLA binary and ternary blends, the fracture surface of the impact specimens was investigated under the SEM and the micrographs are shown in Figure 8. The neat PLA showed a smooth and featureless fracture surface without much deformation, indicating a typical brittle fracture behavior.[33] On the fracture surfaces of the binary blend with 20 wt % PEBA, multiple fracture surfaces replaced the single fracture lines, indicating the impact strength was improved. The toughening effect in this case remained moderate due to the poor compatibility between the phases. Some voids due to the pullout of dispersed PEBA particles were clearly observed, which suggested the poor interfacial adhesion of the PLA and the PEBA phases. In comparison to the PLA/PEBA (80/20) blend, the surface of the blend with 20 wt % EMA-GMA showed increased roughness and some fibrils were discernible on the fracture surfaces. No obvious interface between the different phases was observed, indicating the EMA-GMA had better compatibility with the PLA than PEBA. This good compatibility between the PLA and the EMA-GMA phases can be ascribed to the reactive melt blending process at high temperature.

In case of the ternary blends, more and longer fibril threads were noticed, which served as a clear evidence for the ductile fractures. Especially for the PLA/EMA-GMA/PEBA (70/20/10) blend, significant plastic deformation of the PLA matrix was observed, which was a characteristic of shear yielding. The corresponding amount of plastic deformation was very effectively dissipated the fracture energy, which resulted in greatly improved impact strength at room temperature. The impact fractured surfaces of the ternary blends with 10 and 15 wt % EMA-GMA exhibited morphologies different from that of the blend with 20 wt % EMA-GMA. The dispersed minor PEBA phases were clearly distinguishable from the matrix for the PLA/EMA-GMA/PEBA (70/10/20) and PLA/EMA-GMA/PEBA (70/15/15) blends. The voids resulting from the pullout of dispersed PEBA phases were still clearly observed. The matrix surrounding the voids showed only limited deformation. These results implied that the weak

Table 1. Thermal Properties of the Neat Polymers, the Binary Blends, and the Ternary Blends

samples	$T_{g(PLA)}$ (°C)	T_{cc} (°C)	$T_{c(PLA)}$ (°C)	$\Delta H_{c(PLA)}$ (J/g)	$T_{c(PEBA)}$ (°C)	$\Delta H_{c(PEBA)}$ (J/g)	T_m (°C)	ΔH_m (J/g)
PLA	62.0	98.6	95.6	15.8			168.2	45.3
PLA/EMA-GMA(80/20)	61.0	109.2					169.5	28.9
PLA/PEBA(80/20)	61.2	102.9	92.1	3.6	146.7	0.6	168.5	38.0
PLA/EMA-GMA/PEBA (70/10/20)	61.8	108.5	88.6	6.0	146.4	0.3	169.4	32.4
PLA/EMA-GMA/PEBA (70/20/10)	61.3	109.3	88.5	3.5			169.5	26.3
PEBA(Pebax 55R53)				30.9	151.1	30.3	172.5	36.8

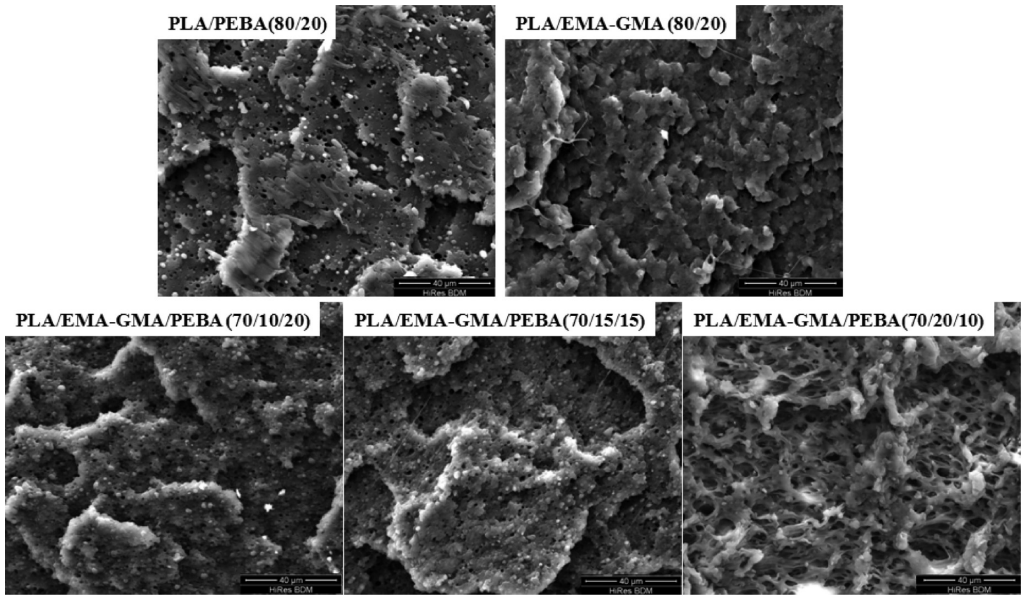

Figure 8. SEM images of impact-fracture surface of the binary blend and PLA/EMA-GMA/PEBA ternary blend with various weight compositions.

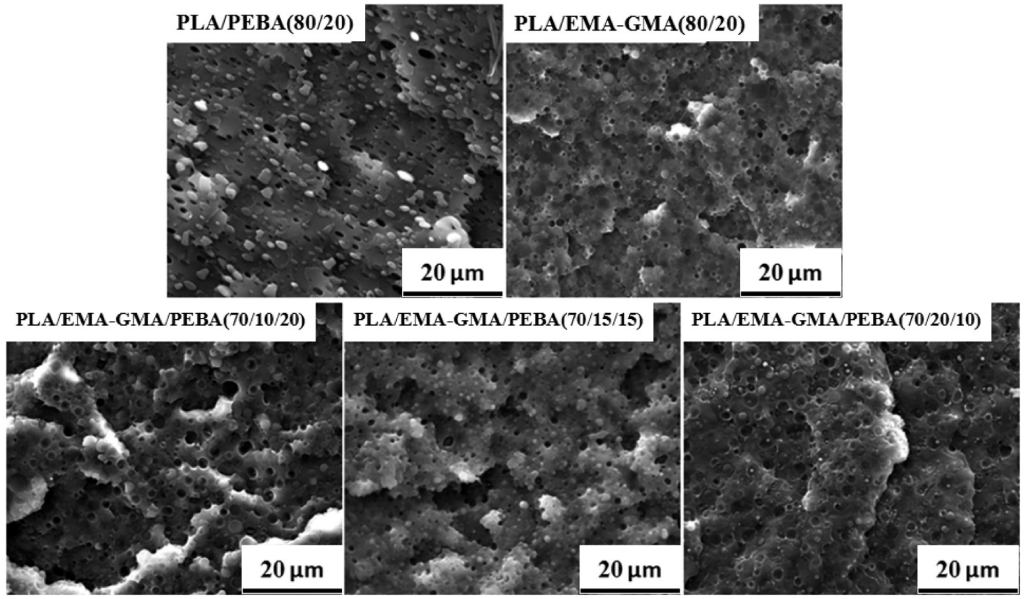

Figure 9. SEM images of cryofractured surface of PLA/EMA-GMA/PEBA blend with various weight compositions.

interfacial adhesion between the dispersed PEBA phases at these particular weight ratios of the blending components lead to similar results as that of the PLA/PEBA binary blend. In contrast, the dispersed particles in the PLA/EMA-GMA/PEBA (70/20/10) were not clearly defined from the PLA matrix. The matrix near the dispersed phases underwent large deformations.

3.5. Phase Morphology of the Blend. It is well-known that the phase morphology has significant influence on the properties of the multiphase blend. As mentioned previously, the ternary blends of the PLA/EMA-GMA/PEBA showed improved mechanical properties compared to the neat PLA and the binary blends. Moreover, the toughness and the flexibility of the ternary blends showed a significant dependence on the composition of the blend components. Therefore, the phase morphology of the ternary blends was studied in an attempt to establish the relationship between the morphology and the resulting performance.

To figure out the toughening mechanism responsible for imparting the supertoughness, the phase morphologies of the binary and the ternary blends were thoroughly studied by the SEM. The SEM images of the cryofractured surface of the PLA binary and the ternary blends with various weight compositions are presented in Figure 9. A clear, phase-separated morphology with the PEBA dispersed in the PLA matrix was observed for the PLA/PEBA binary blend from the SEM results, which indicated that the PLA and PEBA were immiscible. Compared to the PLA/PEBA binary blend, a relatively good interfacial adhesion was found for the PLA/EMA-GMA binary blend, which indicated a good compatibility of the two phases. In a nonreactive ternary blend system with two minor components, generally three different morphologies can be expected and usually reported in the literatures: (1) separate dispersion of the minor phases; (2) stack formation/partial encapsulation; (3) core−shell structure.[25−27] In the SEM micrograph of the PLA/

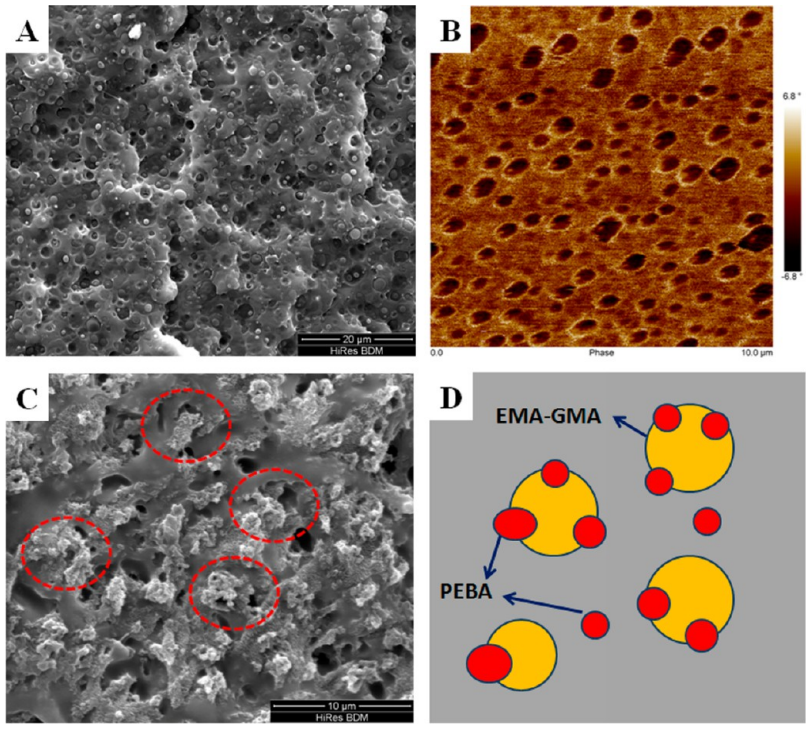

Figure 10. Detail structure of the PLA/EMA-GMA/PEBA (70/20/10) blend with the SEM and AFM phase images: (A) SEM images of cryofractured surface (4000×), (B) AFM image, (C) SEM images of cryofractured surface after etched (10000×), and (D) the schematic structure.

EMA-GMA/PEBA (70/10/20) blend, mainly separate dispersion of the minor phases with large size distribution was the major observation, but a small number of simple single-stacked structures were also observed in the image. It is to be noted that the droplets with larger size showed clear interface with the PLA matrix, which was similar to the appearance of the PEBA particles in the PLA/PEBA binary blend. Considering the composition of this formulation and morphological characters, the larger dispersed particles could be attributed to the PEBA domains. Similarly, separate minor phases with relatively uniform size were observed in the case of the PLA/EMA-GMA/PEBA (70/15/15) blend. On the other hand, for the PLA/EMA-GMA/PEBA (70/20/10) ternary blend exhibiting super high toughness, a special "multiple stack formation" structure with two dispersed polymers stuck together was observed to be the dominant morphology. By referring to the blend morphology as "multiple stack formation" we mean to describe that the dispersed particles are distinctly stuck together in PLA matrix but not necessarily like a stack of coins.

This distinct morphology of the PLA/EMA-GMA/PEBA (70/20/10) blend noticed from AFM and SEM images is represented in Figure 10. Phase image obtained from AFM is usually used to reveal material contrast in polymer blends as it is a precise method to detect the structures in the materials in a nanometer range. Partial encapsultation or the stack formation was also clearly evident from the AFM, corroborating the SEM observations. Multiple dispersed small particles were found to be stuck together in one larger droplet. The SEM and AFM results clearly indicated the unique "multiple stacked structure" formed by the PLA/EMA-GMA/PEBA (70/20/10) formulation. At the same time, as shown in Figure 10A, the large domains seemed to have good interfacial adhesion with the matrix, while the small size particles were detached from the matrix showing distinct interfaces. As discussed in the binary PLA/EMA-GMA blend, the EMA-GMA showed good compatibility with PLA matrix. Therefore, here the larger particles having good interfacial adhesion with the PLA matrix could be attributed to the EMA-GMA, while the small particles with poor interfacial adhesion could be ascribed to the PEBA phase having low content in this formulation. To further clearly distinguish the minor phases, the morphology of the ethched cryofractured surface of the PLA/EMA-GMA/PEBA (70/20/10) blend was also observed under the SEM and the micrograph is shown in Figure 10 (C). During the etching processing, the PEBA phases were selectively etched by the solvent. From Figure 10 (C), the holes, which were ascribed to the etched PEBA phases, can be clearly observed at the interface of the dispersed EMA-GMA and the PLA matrix. Moreover, some voids stacked with the EMA-GMA phases were also observed at the interfaces in the images. This result further confirmed the unique structure of the PLA/EMA-GMA/PEBA (70/20/10) blend.

Several theoretical models have been used to predict the morphology of the ternary polymer blends.[25,49,50] Among these models, spreading coefficient model have been widely used in the literatures. On the basis of the concept of a spreading coefficient, Hobbs et al. successfully predicted the morphology of immiscible polymer ternary blend by rewriting the Harkin's equation.[45]

$$\lambda_{CB} = \alpha_{BA} - \alpha_{CA} - \alpha_{BC}$$

λ_{ij} is the spreading coefficient of i over j and α_{ij} is the interfacial tension between i and ij. For B to be encapsulated by C, λ_{CB} must be positive. In the case when both λ_{CB} and λ_{BC} are negative, B and C will tend to form separated phases. Here, the morphologies of the ternary blends were predicted using the spreading coefficient theory. Since there is no related interfacial tension data for each pairs of the PLA, EMA-GMA, and PEBA are available from the literatures, we have calculated the interfacial tension values based on the surface tension values

Table 2. Interfacial Tension Values at Room Temperature and Extrapolated to 190 °C and Spreading Coefficient

polymer pairs	interfacial tension, γ_{ij} (mN/m) using harmonic mean equation	interfacial tension, γ_{ij} (mN/m) using geometric mean equation	interfacial tension, γ_{ij} (mN/m) at 190 C using geometric mean equation	spreading coefficient, λ_{ij}
PLA/EMA-GMA (γ_{ab})	3.61	1.84	5.91	$\lambda_{bc} = -7.53$
PLA/PEBA (γ_{ac})	1.69	0.85	1.40	$\lambda_{cb} = 1.49$
EMA-GMA/PEBA (γ_{bc})	1.40	0.70	3.01	$\lambda_{ab} = -4.30$

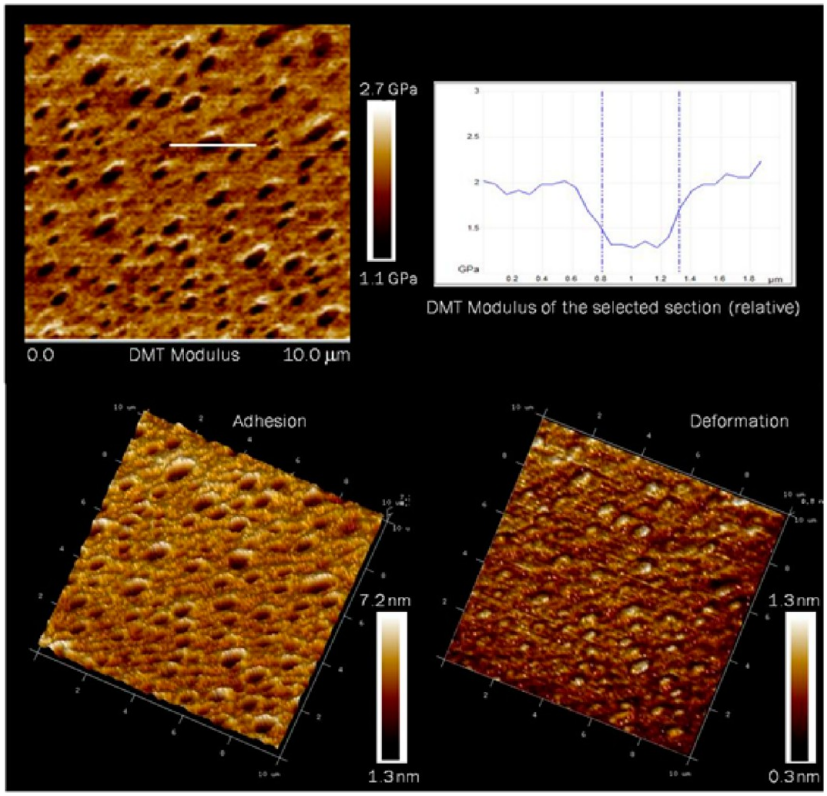

Figure 11. AFM images of PLA/EMA-GMA/PEBA (70/20/10) ternary blend obtained under PeakForce QNM mode.

measured by the contact angle. The contact angle and surface tension values for all the components of the blend can be referred in Support Information Table S1. Since the melt blending was carried out at essentially higher temperatures, the use of interfacial tension values calculated from surface tension values requires to be extrapolated to the processing temperature. To do that, a temperature coefficient of -0.06 mJ m^{-2} K^{-1} was used as adopted in many of the literatures. The interfacial values and spreading coefficient calculated for the polymer pairs are listed in Table 2.

Contrary to our expectation, the theoretical calculations predicted a different morphology that was not consistent with the real morphologies shown in Figure 10. As shown in the table, the spreading coefficient calculated from the extrapolated interfacial tension values reveal complete encapsulation morphology with the PEBA forming the shell and the EMA-GMA forming the core. As these equations are originally proposed for nonreactive blends based on static interfacial tensions, it is important to mention that the predictability is limited in case of the reactive compatibilized blends under shear flowing conditions. It is well-known that the interfacial tensions of polymer pairs can be significantly changed by in situ reaction at the interface during the reactive blending. Fleischer et al. pointed out that the interfacial tension could be reduced up to 70% through the interfacial modification with a end-functionalized interfacial agent.[51] As it can be seen, the interfacial tension values obtained for the PLA/EMA-GMA pair is higher under static nonreactive situation, but in actual fact it would be much lower considering the reaction of the EMA-GMA with the PLA. The same is true for the EMA-GMA/PEBA pair as well. In fact, with the SEM observations, a good interface was found to be present in the PLA/EMA-GMA binary blend in comparison to the PLA/PEBA binary blend, which could be attributed to the reaction of epoxy groups of EMA-GMA with carboxyl groups of the PLA. The DSC and DMA results also suggested that there was improved compatibility between the EMA-GMA and the other components in the blends. The change of interfacial tension and composition under melt processing condition has been widely used to manipulate the morphology of the multiphase blends. In blends of polyamide 6/polycarbonate/poly [styrene-*b*-(ethylene-*co*-butylene)-*b*-styrene], Horiuchi et al. demonstrated that interfacial compatibilization reaction between the components during melt-mixing induces the change of the phase morphology.[27] In a model ternary blend of polyamide, polypropylene and polystyrene, Wang et al.[52] and Omonov et al.[53] both indicated in their

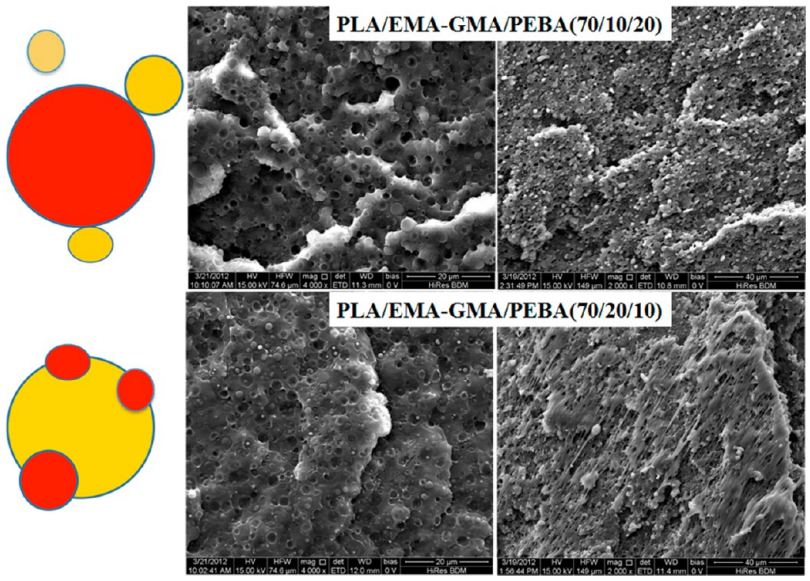

Figure 12. Schematic and impact surface graphs of the blends near the notch.

respective studies that the morphology of the blend has been changed because of the change of interfacial tension by adding the compatibilizer. Therefore, experimental technique measuring the dynamic interfacial tension existing between the polymer pairs may be more useful for the melt compounded reactive systems due to the changed interfacial tension data and influence of shear flow on the delicate balance of interfacial tensions within the blend. In the present PLA/EMA-GMA/PEBA blends, the melt reaction of the EMA-GMA with the PLA and the PEBA will significantly decrease the interfacial tension of the component pairs. Owing to the interfacial reaction, EMA-GMA phases will prefer to be located in the interface between the PLA and the PEBA in the blend. A unique "multiple stack structure" was therefore formed at an appropriate blend ratio of PLA/EMA-GMA/PEBA (70/20/10).

3.6. Toughening Mechanism. It has been widely accepted that the effciency of the elastomer in toughening the polymer blend is significantly dependent on the interfacial adhesion and the cavition process. It is well recognized that the interfacial adhesion between the dispersed domians and matrix play a very delicate role in toughening the blend. To achieve high toughening effect, the dispersed particles should have suitable interfacial adhension with the matrix to improve the phase disperson and to inhibit the crack formation. Poor interfacial adhesion will induce phase segregation and can not afford the crack formation. However, a too strong interfical adhesion usually is not benefical for toughness as it does not allow the stress to be relieved via interfacil debonding. Debonding at the interface between the dispersed patrticles and matrix is an important cause for microvoiding, which is a key step for the innitiation of matrix deformation. In polymer/elastomer blends, the dispersed modifer particles act as stress concentrators as they possesss different elastic properties compared to the matrix. A higher hydrostatic or triaxial stress is applied to the particles, which will result in void formation through internal cavition or debonding. Consequently, a suitable phase structure with optimium interfacial adhesion is very important for the toughening of the polymer/elastomer blends.

As discussed previously, the PLA/EMA-GMA/PEBA (70/20/10) formulation with a unique phase structure compared to other formualtions showed superior impact strength. To establish the toughening mechanism of the blends, AFM PeakForce QNM mode was first used to map the relative DMT modulus of different phases in the blend. Figure 11 shows the 10 μm AFM scan of PLA/EMA-GMA/PEBA (70/20/10) displaying DMT modulus, adhesion and deformation. The softer domains of the PEBA and the EMA-GMA appear darker in the DMT modulus image revealing the realtive modulus of the domains to be ~1.2 GPa and the PLA with ~2.2 GPa as shown in Figure 11. As expected, the PEBA and the EMA-GMA particles dispersed in the blends deformed at a higher rate compared to the PLA matrix, and appeared brigher on the scale bar with a maximum deformation value of 1.3 nm. This difference in elastic properties will be benefical for the microformation during fracture process. Interfacial debonding will be a key step for the initiation of the microformation in the blend.

The impact fractured morphologies of the PLA/EMA-GMA/PEBA (70/10/20) and the PLA/EMA-GMA/PEBA(70/20/10) blends in the vicinity of the notch were further characterized using SEM and are shown in Figure 12. In the PLA/EMA-GMA/PEBA (70/10/20) blend, it was obvious that strong interfacial debonding occurred due to the weak interfacial adhesion of the PEBA particles with the PLA matrix. Detached particles and large voids belonging to the PEBA phase was clearly observed in the image, which was due to the poor interfacial adhension of the PEBA and the PLA phases. During the impact fracutre process, the presence of poor interfacial adhesion promoted the crack formation, which resulted in very limited improvement in the toughness. However, a different deformation phenomema was observed for the PLA/EMA-GMA/PEBA (70/20/10) blend. Similar interfacial debonding was also noticed in the PLA/EMA-GMA/PEBA (70/20/10) blend however a significant difference from the previous PLA/EMA-GMA/PEBA (70/10/20) blend was that the dispersed domains were found to be still adhered to the PLA matrix through small oval cavities. These results indicated that although interfacial debonding occurred between the phases, the balanced interfacial adhesion of the dispersed phases were still high enough to inhibit the crack formation. This different deformation phenomema resulted in completely

different toughness properties and tremendously enhanced the impact strength.

As shown in Figure 10 and Figure 12, the partial wetting of the PEBA on the EMA-GMA partilces resulted in special structure with mutiple PEBA particles stacked with the EMA-GMA particles between the PLA and EMA-GMA interface. From the previous analysis it was clear that the EMA-GMA had good compatibilty with the PLA matrix due to the reactions occurring at high temperature. The good interfacial adhesion of the EMA-GMA particle with the PLA matrix will effectively faciliate the stress transfer during the fracture process, which can prevent the crack initation and propagation. This will help in considerable matrix deformation and result in substanial energey consumption.[30] On the other hand, the mutiple PEBA particels with poor interfacial adhesion located at the interface will weaken the interfacial adhesion to a certain extent. Consequently, during the development of fracture process, interfacial debonding of PEBA particles from the PLA will result in the mutiple microvoid formation, which will easily trigger the deformation of the surrounding matrix. This delicate balance of interfacial adhesion and debonding was believed to play a very positive role in improving the toughenss of PLA matrix. At the same time, the deceased size of the PEBA particles shown in the micrograph will be also beneficial for improving the impact strength.

In PLA-based toughnening blends, a good cooperation of interfacial debonding and suitable level of interfacical adhesion played an important role to improve the toughenss of PLA matrix.[7−11] In a PLA/hyperbranched poly(ester amide) (HBP) blend, Lin et al. also found that the interplay of moderate interfacial H-bonding allowing interfacial debonding between the HBP and PLA phases resulted in high toughness of the materials.[12] Similar effect was also found in a PLA/poly(ether) urethane/titanium dioxide (TiO_2) nanopartiles composites.[54]The selective interfacially localized nano-TiO_2 induced moderately weakend interfacial adhesion, which was benifacial for the interfacial debonding. Recently, in the PLA/natural rubber/Clay biocomposites, Bitinis et al. also found the presence of the nanoclay at the interface of the PLA and the natural rubber phases helping in hindering the formation of voids, which significantly improved the toughness of the composites.[37] Kim et al.[55,56] have proposed that the multiple cavitaion process in the ternary blend systems significantly enhanced the shear flowing in the matrix. Consequently, the complementary role of the PEBA and the EMA-GMA phases in the unique "mutiple stack structure" during the fracture process contributed to superhigh toughenss achieved. This unique phase structures and toughening mechanism also explain the mechancial properteis of PLA/EMA-GMA/PEBA(70/20/10) blend with different grades of PEBA as shown in Figure 4. During the impact process, the stiffness of PEBA had no obvious effect on the interfacial adhesion and debonding in the unique "mutiple stack structure". Consequently, the stiffness of PEBA had no significant influence on the toughness. In summary, a unique synergetic effect of the PEBA and the EMA-GMA phases in the "multiple stacked structure" were believed to contribute the excellent toughness of the blend.

CONCLUSIONS

This Research Article reports on the development of supertough ternary PLA renewable blends with a mixture of morphologies formed by reactive melt blending of the PLA/EMA-GMA/PEBA ternary blends. DMA and DSC analysis revealed that the PLA/PEBA were immiscible, while the PLA/EMA-GMA binary blends showed partial miscibility. Significant enhancement of the toughness of the PLA was achieved by the ternary blend of PLA/EMA-GMA/PEBA. Supertough PLA ternary blend exhibiting the impact strength of ∼500 J/m, with partial break impact behavior was obtained by optimizing the blending ratio at 20 wt % EMA-GMA and 10 wt % PEBA. Different phase morphologies were manipulated by interfacial reaction and composition changing of the ternary blends. A unique "multiple stacked structure" with partial encapsulation of the EMA-GMA and the PEBA minor phases was observed for the PLA/EMA-GMA/PEBA (70/20/10). Morphological studies showed that synergistic effect of good interfacial adhesion and interfacial cavitations followed by massive shear yielding of the PLA matrix contributed to the enormous toughening effect observed in the ternary blends.

ASSOCIATED CONTENT

Supporting Information

Contact angle and surface tension values calculated for individual blend components are given in the Supporting Information, Table S1. This material is available free of charge via the Internet at http://pubs.acs.org.

AUTHOR INFORMATION

Corresponding Authors

*E-mail: mmisra@uoguelph.ca.

*E-mail: mohanty@uoguelph.ca. Tel.: +1 519 824 4120, ext. 56664. Fax: +1 519 763 8933.

Notes

The authors declare no competing financial interest.

ACKNOWLEDGMENTS

The authors are grateful for the financial support from (1) the Ontario Ministry of Agriculture, Food, and Rural Affairs (OMAFRA)—New Directions and Alternative Renewable Fuels research program; (2) the Ontario Ministry of Economic Development and Innovation (MEDI), Ontario Research Fund—Research Excellence Round 4 program and (3) the Natural Sciences and Engineering Research Council (NSERC), Canada NCE AUTO21 program.

REFERENCES

(1) Yu, L.; Dean, K.; Li, L. Polymer Blends and Composites from Renewable Resources. *Prog. Polym. Sci.* **2006**, *36*, 576−602.

(2) Williams, C. K.; Hillmyer, M. A. Polymers from Renewable Resources: A Perspective for a Special Issue of Polymer Reviews. *Polym. Rev.* **2008**, *48*, 1−10.

(3) Lim, L. T.; Auras, R.; Rubino, M. Processing Technologies for Poly(Lactic Acid). *Prog. Polym. Sci.* **2008**, *33*, 820−852.

(4) Drumright, R. E.; Gruber, P. R.; Henton, D. E. Polylactic Acid Technology. *Adv. Mater.* **2000**, *12*, 1841−1846.

(5) Auras, R.; Harte, B.; Selke, S. An Overview of Polylactides as Packaging Materials. *Macromol. Biosci.* **2004**, *4*, 835−864.

(6) Anderson, K. S.; Schreck, K. M.; Hillmyer, M. A. Toughening Polylactide. *Polym. Rev.* **2008**, *48*, 85−108.

(7) Liu, H.; J. Zhang, J. Research Progress in Toughening Modification of Poly (lactic acid). *J. Polym. Sci., Part B: Polym. Phys.* **2011**, *49*, 1051−1083.

(8) Kfoury, G.; Raquez, J.; Hassouna, F.; Odent, J.; Toniazzo, V.; Ruch, D.; Dubois, P. Recent Advances in High Performance Poly(Lactide): From "Green" Plasticization to Super-tough Materials via (Reactive) Compounding. *Front. Chem.* **2013**, *1*, 1−45.

(9) Jiang, L.; Wolcott, M. P.; Zhang, J. Study of Biodegradable Polylactide/Poly(Butylenes Adipate-co-terephthalate) Blends. *Biomacromolecules* **2006**, *7*, 199−207.
(10) Anderson, K. S.; Lim, S. H.; Hillmyer, M. A. Toughening of Polylactide by Melt Blending with Linear Low-Density Polyethylene. *J. Appl. Polym. Sci.* **2003**, *89*, 3757−3768.
(11) Anderson, K. S.; Hillmyer, M. A. The Influence of Block Copolymer Microstructure on the Toughness of Compatibilized Polylactide/Polyethylene Blends. *Polymer* **2004**, *45*, 8809−8823.
(12) Lin, Y.; Zhang, K. Y.; Dong, Z. M.; Dong, L. S.; Li, Y. S. Study of Hydrogen-Bonded Blend of Polylactide with Biodegradable Hyperbranched Poly(Ester Amide). *Macromolecules* **2007**, *40*, 6257−6267.
(13) Li, Y. J.; Shimizu, H. Toughening of Polylactide by Melt Blending with a Biodegradable Poly(Ether)urethane Elastomer. *Macromol. Biosci.* **2007**, *7*, 921−928.
(14) Bhardwaj, R.; Mohanty, A. K. Modification of Brittle Polylactide by Novel Hyperbranched Polymer-Based Nanostructures. *Biomacromolecules* **2007**, *8*, 2476−2484.
(15) Hashima, K.; Nishitsuji, S.; Inoue, T. Structure-Properties of Super-Tough PLA Alloy with Excellent Heat Resistance. *Polymer* **2010**, *51*, 3934−3939.
(16) Oyama, H. T. Super-Tough Poly(Lactic Acid) Materials: Reactive Blending with Ethylene Copolymer. *Polymer* **2009**, *50*, 747−751.
(17) Zhang, K.; Ran, X.; Wang, X.; Han, C.; Han, L.; Wen, X.; Zhuang, Y.; Dong, L. Improvement in Toughness and Crystallization of Poly(L-Lactic Acid) by Melt Blending with Poly(Epichlorohydrin-co-ethylene oxide). *Polym. Eng. Sci.* **2011**, *51*, 2370−2380.
(18) Broz1, M. E.; VanderHart, D. L.; Washburn, N. R. Structure and Mechanical Properties of Poly(D,L-Lactic Acid)/Poly(ε-Caprolactone) Blends. *Biomaterials* **2003**, *24*, 4181−4190.
(19) Robertson, M. L.; Chang, K.; Gramlich, W. M.; Hillmyer, M. A. Toughening of Polylactide with Polymerized Soybean Oil. *Macromolecules* **2010**, *43*, 1807−1814.
(20) Noda, I.; Satkowski, M. M.; Dowrey, A. E.; Marcott, C. Polymer Alloys of Nodax Copolymers and Poly(Lactic Acid). *Macromol. Biosci.* **2004**, *4*, 269−275.
(21) Shibata, M.; Inoue, Y.; Miyoshi, M. Mechanical Properties, Morphology, and Crystallization Behavior of Blends of Poly(L-Lactide) with Poly(Butylene Succinate-co-L-lactate) and Poly(butylene succinate). *Polymer* **2006**, *47*, 3557−3564.
(22) Lu, J. M.; Qiu, Z. B.; Yang, W. T. Fully Biodegradable Blends of Poly(L-Lactide) and Poly(Ethylene Succinate): Miscibility, Crystallization, and Mechanical properties. *Polymer* **2007**, *48*, 4196−4204.
(23) Ojijo, V.; Ray, S. S.; Sadiku, R. Toughening of Biodegradable Polylactide/Poly(Butylene Succinate-co-adipate) Blends via in Situ Reactive Compatibilization. *ACS Appl. Mater. Interfaces* **2013**, *5*, 4266−4276.
(24) Luzinov, I.; Pagnoulle, C.; Jerome, R. Ternary Polymer Blend with Core−Shell Dispersed Phases: Effect of the Core-forming Polymer on Phase Morphology and Mechanical Properties. *Polymer* **2000**, *41*, 7099−7109.
(25) Ticiane, S. V.; Augusto, T. M.; Nicole, R. D. Study of Morphologies of PMMA/PP/PS Ternary Blends. *Macromolecules* **2006**, *39*, 2663−2675.
(26) Joe, R.; Basil, D. F. Control of the Subinclusion Microstructure in HDPE/PS/PMMA Ternary Blends. *Macromolecules* **2000**, *33*, 6998−7008.
(27) Horiuchi, S.; Matchariyakul, N.; Yase, K.; Kitano, T. Morphology Development through an Interfacial Reaction in Ternary Immiscible Polymer Blends. *Macromolecules* **1997**, *30*, 3664−3670.
(28) Li, Y.; Shimizu, H. Compatibilization by Homopolymer: Significant Improvements in the Modulus and Tensile Strength of PPC/PMMA Blends by the Addition of a Small Amount of PVAc. *ACS Appl. Mater. Interfaces* **2009**, *1*, 1650−1655.
(29) Li, L.; Yin, B.; Zhou, Y.; Gong, L.; Yang, M.; Xie, B.; Chen, C. Characterization of PA6/EPDM-g-MA/HDPE Ternary Blends: The Role of Core−Shell Structure. *Polymer* **2012**, *53*, 3043−3051.
(30) Yin, B.; Li, L.; Zhou, Y.; Gong, L.; Yang, M.; Xie, B. Largely Improved Impact Toughness of PA6/EPDM-g-MA/HDPE Ternary Blends: The Role of Core−shell Particles Formed in Melt Processing on Preventing Micro-crack Propagation. *Polymer* **2013**, *54*, 1938−1947.
(31) Liu, H.; Chen, F.; Liu, B.; Estep, G.; Zhang, J. Super Toughened Poly(Lactic Acid) Ternary Blends by Simultaneous Dynamic Vulcanization and Interfacial Compatibilization. *Macromolecules* **2010**, *43*, 6058−6066.
(32) Liu, H.; Song, W.; Chen, F.; Guo, L.; Zhang, J. Interaction of Microstructure and Interfacial Adhesion on Impact Performance of Polylactide (PLA) Ternary Blends. *Macromolecules* **2011**, *44*, 1513−1522.
(33) Zhang, K.; Mohanty, A. K.; Misra, M. Fully Biodegradable and Biorenewable Ternary Blends from Polylactide, Poly(3-Hydroxybutyrate-co-hydroxyvalerate) and Poly(Butylene Succinate) with Balanced Properties. *ACS Appl. Mater. Interfaces* **2012**, *4*, 3091−3101.
(34) Ravati, S.; Favis, B. D. Tunable Morphologies for Ternary Blends with Poly(Butylene Succinate): Partial and Complete Wetting Phenomena. *Polymer* **2013**, *54*, 3271−3281.
(35) Ravati, S.; Favis, B. D. Interfacial Coarsening of Ternary Polymer Blends with Partial and Complete Wetting Structures. *Polymer* **2013**, *54*, 6739−6751.
(36) Bitinis, N.; Verdejo, R.; Cassagnau, P.; Lopez-Manchado, M. A. Structure and properties of polylactide/natural rubber blends. *Mater. Chem. Phys.* **2011**, *129*, 823−831.
(37) Bitinis, N.; Sanz, A.; Nogales, A.; Verdejo, R.; Lopez-Manchado, M. A.; Ezquerra, T. A. Deformation Mechanisms in Polylactic Acid/Natural Rubber/Organoclay Bionanocomposites as Revealed by Synchrotron X-ray Scattering. *Soft Matter* **2012**, *8*, 8990−8997.
(38) Bitinis, N.; Verdejo, R.; Maya, E. M.; Espuche, E.; Cassagnau, P.; Lopez-Manchado, M. A. Physicochemical Properties of Organoclay Filled Polylactic Acid/Natural Rubber Blend Bionanocomposites. *Compos. Sci. Technol.* **2012**, *72*, 305−313.
(39) Bitinis, N.; Fortunati, E.; Verdejo, R.; Bras, Julien; Kenny, J. M.; Torre, L.; Lopez-Manchado, M. A. Poly(Lactic Acid)/Natural Rubber/Cellulose Nanocrystal Bionanocomposites. Part II: Properties Evaluation. *Carbohydr. Polym.* **2013**, *96*, 621−627.
(40) Arkema Inc. Products Websites: Pebax Rnew. http://www.pebax.com/en/pebax-range/product-viewer/Pebax-Rnew/ (accessed on Apr 16, 2014).
(41) Sheth, J. P.; Xu, J. N.; Wilkes, G. L. Solid State Structure−Property Behavior of Semicrystalline Poly(Ether-Block-Amide) PEBAX Thermoplastic Elastomers. *Polymer* **2003**, *44*, 743−756.
(42) Eustache, R. P. In *Handbook of Condensation Thermoplastic Elastomer*; Fakirov, S., Eds; Wiley-VCH: Verlag GmbH & Co. KGaA: Weinheim, Germany, 2005; Chapter 10, pp 263−280.
(43) Zhang, W.; Chen, L.; Zhang, Y. Surprising Shape-memory Effect of Polylactide Resulted from Toughening by Polyamide Elastomer. *Polymer* **2009**, *50*, 1311−1315.
(44) Han, L.; Han, C.; Dong, L. Effect of Crystallization on Microstructure and Mechanical Properties of Poly[(Ethylene Oxide)-block-(amide-12)]-toughened Poly(Lactic Acid) Blend. *Polym. Int.* **2013**, *62*, 295−303.
(45) Han, L.; Han, C.; Dong, L. Morphology and Properties of the Biosourced Poly(Lactic Acid)/Poly(Ethylene Oxide-b-amide-12) Blends. *Polym. Compos.* **2013**, *34*, 122−130.
(46) Dong, W.; Jiang, F.; Zhao, L.; You, J.; Cao, X.; Li, Y. PLLA Microalloys Versus PLLA Nanoalloys: Preparation, Morphologies, and Properties. *ACS Appl. Mater. Interfaces* **2012**, *4*, 3667−3675.
(47) Feng, Y.; Zhao, G.; Yin, J.; Jiang, W. Reactive Compatibilization of High-Impact Poly(Lactic Acid)/Ethylene Copolymer Blends Catalyzed by *N*,iN-dimethylstearylamine. *Polym. Int.* **2013**, DOI: 10.1002/pi.4632.
(48) Martin, P.; Devaux, L.; Legras, R.; van Gurp, M.; van Duin, M. Competitive Reactions during Compatibilization of Blends of Polybutyleneterephthalate with Epoxide-containing rubber. *Polymer* **2001**, *42*, 2463−2478.

(49) Hobbs, S. Y.; Dekkers, M. E. J.; Watkins, V. H. Effect of Interfacial Forces on Polymer Blend Morphologies. *Polymer* **1988**, *29*, 1598−1602.
(50) Guo, H.; Packirisamy, S.; Gvozdic, N. V.; Meier, D. J. Prediction and Manipulation of the Phase Morphologies of Multiphase Polymer Blends: 1. Ternary Systems. *Polymer* **1997**, *38*, 785−794.
(51) Fleischer, C. A.; Morales, A. R.; Koberstein, J. T. Interfacial Modification through End Group Complexation in Polymer Blends. *Macromolecules* **1994**, *27*, 379−385.
(52) Wang, D.; Li, Y.; Xie, X.; Guo, B. Compatibilization and Morphology Development of Immiscible Ternary Polymer Blends. *Polymer* **2011**, *52*, 191−200.
(53) Omonov, T. S.; Harrats, C.; Groeninckx, G. Co-continuous and Encapsulated Three Phase Morphologies in Uncompatibilized and Reactively Compatibilized Polyamide 6/Polypropylene/Polystyrene Ternary Blends Using Two Reactive Precursors. *Polymer* **2005**, *46*, 12322−12336.
(54) Xiu, H.; Bai, H.; Huang, M.; Xu, C.; Li, X.; Fu, Q. Selective Localization of Titanium Dioxide Nanoparticles at the Interface and its Effect on the Impact Toughness of Poly(L-Lactide)/Poly(Ether)-urethane Blends. *Express Polym. Lett.* **2013**, *7*, 261−271.
(55) Kim, G.; Michler, G. Micromechanical Deformation Processes in Toughened and Particle Filled Semicrystalline Polymers: Part 2. Model Representation for Micromechanical Deformation Processes. *Polymer* **1998**, *39*, 5699−5703.
(56) Kim, G.; Michler, G. Micromechanical Deformation Processes in Toughened and Particle-filled Semicrystalline Polymers: Part 1. Characterization of Deformation Processes in Dependence on Phase Morphology. *Polymer* **1998**, *39*, 5689−5697.